Synthesis, Structures, Dynamics, and Ethylene Polymerization Activity of Nickel Complexes Containing an *ortho*-Methoxy-aryl Diphosphine Ligand

Laurent Lavanant,[‡] Anne-Sophie Rodrigues,[‡] Evgueni Kirillov,[‡] Jean-François Carpentier,*[,‡] and Richard F. Jordan*[,§]

Sciences Chimiques de Rennes, UMR 6226 CNRS−Université de Rennes 1, 35402 Rennes, Cedex, France, and Department of Chemistry, The University of Chicago, 5735 S. Ellis Avenue, Chicago, Illinois 60637

Received December 3, 2007

The Ni coordination chemistry of {(2-OMe-4-Me-Ph)$_2$P}$_2$NMe (**2**, PNP) has been studied. The reaction of (dimethoxyethane)NiBr$_2$ with **2** yields {PNP}NiBr$_2$ (**3**, 75%). The reaction of Ni(cod)$_2$ (cod = 1,5-cyclooctadiene) with 2 equiv of **2** affords {PNP}$_2$Ni (**4**, 61%). The reaction of Ni(cod)$_2$ with 1 equiv of **2** yields {PNP}Ni(cod) (**5**, 90%) via initial formation of **4** (50%), followed by comproportionation with Ni(cod)$_2$. X-ray crystallographic analyses of **3** and **4** show that the methoxy groups do not coordinate to Ni but reveal the presence of weak CH---Ni interactions involving the *ortho* aryl hydrogens, and weak CH$-\pi$ interactions involving the OMe hydrogens and the aryl rings. The reaction of **5** with [H(OEt$_2$)$_2$][B(3,5-(CF$_3$)$_2$C$_6$H$_3$)$_4$] or [H(OEt$_2$)$_2$][B(C$_6$F$_5$)$_4$] generates a cationic species formulated as {PNP}Ni(codH)$^+$ (**6**) on the basis of ESI-MS data. Cation **6**, generated *in situ* from Ni(cod)$_2$/**2**/[H(OEt$_2$)$_2$][B(3,5-(CF$_3$)$_2$C$_6$H$_3$)$_4$] or **5**/[H(OEt$_2$)$_2$][B(C$_6$F$_5$)$_4$], catalyzes ethylene polymerization.

Introduction

A variety of *ortho*-alkoxy-aryl phosphine ligands that exhibit interesting properties in catalysis have been described recently (Chart 1). For example, Ni(II) complexes of *o*-MeO-dppe or *o*-MeO-dppp catalytically hydrogenate 1-octene, while analogous nonsubstituted dppe or dppp complexes are inactive.[1] Pd(II) catalysts containing {bis(*ortho*-alkoxyaryl)phosphino}arene sulfonate ligands (PO$^-$), introduced by Pugh and co-workers, catalyze nonalternating ethylene/CO copolymerization to ethylene-enriched polyketones,[2] ethylene/alkyl acrylate copolymerization to linear copolymers with in-chain acrylate incorporation,[3] and other unusual copolymerizations.[4] Consiglio et al. showed that palladium catalysts containing *ortho*-methoxy-substituted arylphosphine-oxazole ligands (PN) catalyze regioirregular alternating styrene/CO copolymerization.[5] Wass et al. reported that chromium complexes of aminodiphosphine ligands that contain *ortho*-methoxyaryl groups (PNP^{OMe}) are active and selective catalyst precursors for ethylene trimerization and tetramerization[6] and for the cotrimerization of ethylene and styrenic comonomers.[7] Additionally, *in situ*-generated Ni(II) complexes containing these (PNP^{OMe}) ligands exhibit better performance in ethylene polymerization and oligomerization than their nonsubstituted analogues.[8]

In several cases, the enhancements of catalytic activity and/or selectivity engendered by the *ortho*-methoxy groups in aryl phosphine ligands have been proposed to arise from steric effects,[4a] because similar enhancements were observed for analogous *ortho*-alkyl-substituted aryldiphosphines.[1c,4e,5,9] In other cases, it was proposed that the *ortho*-methoxy groups act

* Corresponding author. E-mail: jean-francois.carpentier@univ-rennes1.fr, rfjordan@uchicago.edu.

‡ University of Rennes.

§ University of Chicago.

(1) (a) Angulo, I. M.; Kluwer, A. M.; Bouwman, E. *Chem. Commun.* **1998**, 2689. (b) Bouwman, E.; Henderson, R. K.; Powel, A. K.; Reedijk, J.; Smeets, W. J. J.; Veldman, N.; Wocadlo, S. *J. Chem. Soc., Dalton Trans.* **1998**, 3495. (c) Angulo, I. M.; Bouwman, E.; Lok, S. M.; Lutz, M.; Mul, W. P.; Spek, A. L. *Eur. J. Inorg. Chem.* **2001**, 1465. (d) Angulo, I. M.; Bouwman, E.; Lutz, M.; Mul, W. P.; Spek, A. L. *Inorg. Chem.* **2001**, *40*, 2073. (e) Angulo, I. M.; Bouwman, E. *J. Mol. Catal. A: Chem.* **2001**, *175*, 65. (f) Angulo, I. M.; Lok, S. M.; Quiroga Norambuena, V. F.; Lutz, M.; Spek, A. L.; Bouwman, E. *J. Mol. Catal. A: Chem.* **2002**, *187*, 55. (g) Angulo, I. M.; Bouwman, E.; van Gorkum, R.; Lok, S. M.; Lutz, M.; Spek, A. L. *J. Mol. Catal. A: Chem.* **2003**, *202*, 97.

(2) (a) Drent, E.; van Dijk, R.; van Ginkel, R.; van Oort, B.; Pugh, R. I. *Chem. Commun.* **2002**, 964. (b) Drent, E.; Pello, D. H. L. Eur. Pat. Appl. EP0632084 (to Shell), 1995. (c) Hearley, A. K.; Nowack, R. J.; Rieger, B. *Organometallics* **2005**, *24*, 2755. See also. (d) Verspui, G.; Schanssema, F.; Sheldon, R. A. *Angew. Chem., Int. Ed.* **2000**, *39*, 804. (e) Dossett, S. J.; Gillon, A.; Orpen, A. G.; Fleming, J. S.; Pringle, P. G.; Wass, D. F.; Jones, M. D. *Chem. Commun.* **2001**, 699. (f) Kochi, T.; Yoshimura, K.; Nozaki, K. *Dalton Trans.* **2006**, 25. (g) Newsham, D. K.; Borkar, S.; Sen, A.; Conner, D. M.; Goodall, B. L. *Organometallics* **2007**, *26*, 3636.

(3) Drent, E.; van Dijk, R.; van Ginkel, R.; van Oort, B.; Pugh, R. I. *Chem. Commun.* **2002**, 744.

(4) (a) Kochi, T.; Nakamura, A.; Ida, H.; Nozaki, K. *J. Am. Chem. Soc.* **2007**, *129*, 7770. (b) Skupov, K. M.; Marella, P. M.; Hobbs, J. L.; McIntosh, L. H.; Goodall, B. L.; Claverie, J. P. *Macromolecules* **2006**, *39*, 4279. (c) Liu, S.; Borkar, S.; Newsham, D.; Yennawar, H.; Sen, A. *Organometallics* **2007**, *26*, 210. (d) Kochi, T.; Noda, S.; Yoshimura, K.; Nozaki, K. *J. Am. Chem. Soc.* **2007**, *129*, 8948. (e) Luo, S.; Vela, J.; Lief, G. R.; Jordan, R. F. *J. Am. Chem. Soc.* **2007**, *129*, 8946. (f) Weng, W.; Shen, E.; Jordan, R. F. *J. Am. Chem. Soc.* **2007**, *129*, 15450.

(5) Aeby, A.; Gsponer, A.; Consiglio, G. *J. Am. Chem. Soc.* **1998**, *120*, 11000.

(6) (a) Carter, A.; Cohen, S. A.; Cooley, N. A.; Murphy, A.; Scutt, J.; Wass, D. F. *Chem. Commun.* **2002**, 858. (b) Wass,D. F. Pat WO 2002004119, 2002 (to British Petroleum Chemicals). (c) Agapie, T.; Schofer, S. J.; Labinger, J. A.; Bercaw, J. E. *J. Am. Chem. Soc.* **2004**, *126*, 1304. (d) Overett, M. J.; Blann, K.; Bollmann, A.; Dixon, J. T.; Hess, F.; Killian, E.; Maumela, H.; Morgan, D. H.; Neveling, A.; Otto, S. *Chem. Commun.* **2005**, 622. (e) Schofer, S. J.; Day, M. W.; Henling, L. M.; Labinger, J. A.; Bercaw, J. E. *Organometallics* **2006**, *25*, 2743. (f) Agapie, T.; Day, M. W.; Henling, L. M.; Labinger, J. A.; Bercaw, J. E. *Organometallics* **2006**, *25*, 2733. (g) Bollmann, A.; Maumela, H.; Blann, K. Pat. WO 2005123884 2005 (to Sasol Tech.).

(7) Bowen, L. E.; Wass, D. F. *Organometallics* **2006**, *25*, 555.

(8) Wass, D. F. Pat WO 0110876, 2001 (to British Petroleum Chemicals).

(9) Dennett, J. N. L.; Gillon, A. L.; Heslop, K.; Hyett, D.; Fleming, J. S.; Lloyd-Jones, C. E.; Orpen, A. G.; Pringle, P. C.; Wass, D. F. *Organometallics* **2004**, *23*, 6077.

10.1021/om701215s CCC: $40.75
Publication on Web 04/05/2008

Chart 1. Examples of *ortho*-Methoxy-Substituted Diphosphine Ligands Useful in Catalysis

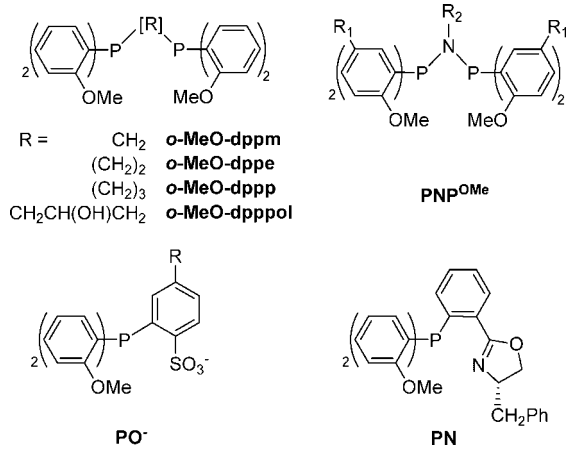

as hemilabile ligands and reversibly coordinate to the metal center during catalysis.[6a,c,10,11] A better understanding of the properties of *ortho*-alkoxy-arylphosphines may enable new opportunities in catalysis.

Here we report initial studies of the synthesis, structures, dynamics, and reactivity of a series of nickel complexes containing a Wass-type PNP^{OMe} aminodiphosphine ligand.

Results and Discussion

Ligand Synthesis. The ligand $\{(2\text{-OMe-4-Me-Ph})_2P\}_2NMe$ (**2**, PNP) was prepared in 52% overall yield using the procedure in Scheme 1, which was adapted from Wass' synthesis of the parent $\{(2\text{-OMe-Ph})_2P\}_2NMe$ compound.[6a] The use of PBr_3 instead of PCl_3 in combination with the ArMg*Br* reagent prevents the formation of a mixture of $(Ar)_2PBr$ (**1**) and $(Ar)_2PCl$ and facilitates the isolation of intermediate **1**.[6a] Reaction of 2 equiv of **1** with methylamine in the presence of triethylamine affords pure **2** as a white solid.

Synthesis of {PNP}NiBr$_2$ (3). The reaction of **2** with $(dme)NiBr_2$ (dme = dimethoxyethane) affords $\{PNP\}NiBr_2$ (**3**) in 75% yield as a red, air-stable, crystalline powder (eq 1). Complex **3** is insoluble in benzene and toluene but is soluble in CH_2Cl_2.

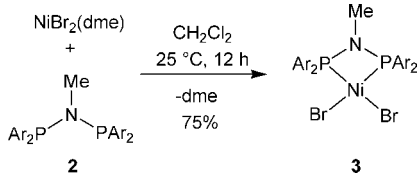

(1)

Molecular Structure of 3. The molecular structure of **3** was determined by X-ray diffraction. Crystal data and selected bond lengths and angles are listed in Tables 1 and 2. The unit cell of **3** contains two independent molecules (**Ni(1)** and **Ni(2)**, see Figure 1) that differ subtly in the conformation of the aryl rings and because they are approximate mirror images. Only the structure of the **Ni(1)** site will be discussed; the structure of the **Ni(2)** site is similar.

Scheme 1

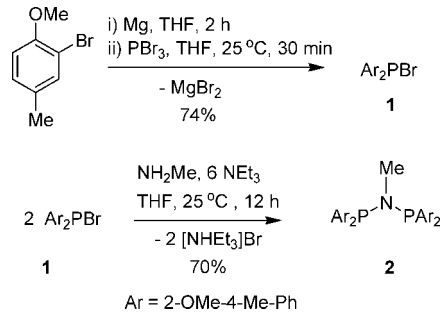

Table 1. Crystal Data and Structure Refinement for {PNP}NiBr$_2$ (3) and {PNP}$_2$Ni (4)

	3	4
formula	$C_{33}H_{39}Br_2NNiO_4P_2 \cdot 1.5CH_2Cl_2$	$C_{66}H_{78}N_2NiO_8P_4 \cdot 4C_7H_8$
fw	1843.02	1578.43
cryst syst	monoclinic	monoclinic
space group	$P2_1/c$	$I2/A$
a, Å	20.072(5)	26.3678(8)
b, Å	18.123(4)	15.4778(6)
c, Å	21.659(5)	23.0880(8)
β, deg	90.563(4)	116.328(2)
V, Å^3	7879(3)	8445.2(5)
Z	4	4
T, K	100(2)	120(1)
cryst color, habit	purple blocks	orange blocks
goodness of fit	0.918	1.046
R (all data)	0.0485	0.1037
wR_2 (all data)	0.0751	0.1632
R [$I > 2\sigma(I)$]	0.0327	0.0606
wR_2 [$I > 2\sigma(I)$]	0.0723	0.1387

The geometry at **Ni(1)** is distorted square planar. The main distortions are the acute P(1)−Ni−P(2) angle (73.07(4)°), which results from the small bite angle of the PNP ligand, and the nonzero dihedral angle between the Br−Ni−Br and P−Ni−P planes (11.50°), which indicates a slight twisting toward tetrahedral geometry. The aryl rings of **3** are oriented in an approximate C_2-symmetric edge/face arrangement. Rings Ar(1) and Ar(4) (see Figure 1) are oriented such that their OMe groups point toward the Ni(1) center. However, the Ni(1)−O(1) (3.609(3) Å) and Ni(1)−O(4) (3.662(2) Å) distances are much greater than the sum of the Ni and O van der Waals radii (3.15 Å),[12] and therefore there are no significant O---Ni interactions. Ar(2) and Ar(3) are rotated 64.56(2)° and 66.11(2)° relative to Ar(1) and Ar(4), respectively, and their OMe groups point toward the NMe side of the molecule. The orientations of the aryl rings can be specified by the Ni−P−C(*ipso*P)−C(*ipso*O) dihedral angles (α), which are listed in Table 3 for Ni(1) and Ni(2).

Close inspection of the structure of **3** reveals that three types of weak interactions are associated with the arrangement of the aryl groups. First, the *ortho* hydrogens in Ar(2) (H(10)) and Ar(3) (H(19)) point toward the nickel center. The Ni---H distances (Ni(1)---H(10) 2.84; Ni(1)---H(19) 2.83 Å)[13] are only slightly longer than the sum of the Ni and H van der Waals radii (2.73 Å). These Ni---H contacts suggest the presence of either agostic interactions or Ni---H−C hydrogen bonds, which have been observed previously in square-planar d^8 ML_4 complexes.[14] In **3**, the Ni−C_{ortho} distances involved in the Ni---HC interaction (Ni(1)---C(19), 3.403(4); Ni(1)---C(10), 3.416(4) Å) are longer than those observed for γ-C---H agostic interactions (Ni---C, 2.30 Å) in related systems.[15] Therefore, we favor a Ni---H−C hydrogen bond model involving the occupied d_{z^2} orbital.[16] A second type of weak interaction in **3** is a OCH−π interaction[17] involving the OCH_3 hydrogens and the aryl rings Ar(2) and Ar(3). The OCH---(Ar centroid) distances (H(8B)---

(10) Slone, C. S.; Weinberger, D. A.; Mirkin, C. A. *Prog. Inorg. Chem.* **1999**, *48*, 233.

(11) For the use of methoxy-aryl phosphine ligands in nickel-catalyzed asymmetric hydrovinylation of olefins, see: (a) Nomura, N.; Jin, J.; Park, H.; Rajanbabu, T. V. *J. Am. Chem. Soc.* **1998**, *120*, 459. (b) Nandi, M.; Jin, J.; Rajanbabu, T. V. *J. Am. Chem. Soc.* **1999**, *121*, 9899.

Table 2. Selected Bond Distances (Å) and Angles (deg) for the Two Independent Molecules (Ni(1) and Ni(2)) in {PNP}NiBr$_2$ (3)

Ni(2)		Ni(1)	
P(4)−N(2)	1.684 (3)	P(1)−N(1)	1.691 (3)
P(3)−N(2)	1.687 (3)	P(2)−N(1)	1.686 (3)
P(4)−Ni(2)	2.1374 (11)	P(1)−Ni(1)	2.1256 (11)
P(3)−Ni(2)	2.1326 (11)	P(2)−Ni(1)	2.1326 (11)
P(3)−P(4)	2.5400 (13)	P(1)−P(2)	2.5352 (13)
Ni(2)−Br(4)	2.336 (7)	Ni(1)−Br(1)	2.338 (7)
Ni(2)−Br(3)	2.349 (7)	Ni(1)−Br(2)	2.332 (7)
P(3)−N(2)−P(4)	97.79 (14)	P(1)−N(1)−P(2)	97.31 (14)
P(3)−Ni(2)−P(4)	73.00 (4)	P(1)−Ni(1)−P(2)	73.07 (4)
Br(3)−Ni(2)−Br(4)	98.77 (2)	Br(1)−Ni(1)−Br(2)	98.59 (2)
P(3)−Ni(2)−Br(3)	95.58 (2)	P(1)−Ni(1)−Br(1)	94.03 (3)
P(4)−Ni(2)−Br(4)	94.24 (3)	P(2)−Ni(1)−Br(2)	95.32 (3)
P(4)−Ni(2)−Br(3)	164.27 (3)	P(1)−Ni(1)−Br(2)	165.32 (3)
P(3)−Ni(2)−Br(4)	163.56 (3)	P(2)−Ni(1)−Br(1)	164.83 (3)
H(41B)-Ar(7)	2.66	H(33B)−Ar(2)	2.61
H(65B)-Ar(6)	2.66	H(8B)−Ar(3)	2.67
H(51)−Ni(2)	2.82	H(10)−Ni(1)	2.84
H(43)−Ni(2)	2.93	H(19)−Ni(1)	2.83
C(51)−Ni(2)	3.403 (4)	C(10)−Ni(1)	3.416 (4)
C(43)−Ni(2)	3.453 (4)	C(19)−Ni(1)	3.403 (4)
O(5)−Ni(2)	3.748 (2)	O(1)−Ni(1)	3.609 (3)
O(8)−Ni(2)	3.615 (3)	O(4)−Ni(1)	3.662 (2)
C(51)−H(51)−Ni(2)	120.60	C(19)−H(19)−Ni(1)	119.85
C(43)−H(43)−Ni(2)	115.69	C(11)−H(1)−Ni	115.89
O(6)−H(66A)	2.33	O(3)−H(17A)	2.30
O(7)−H(66B)	2.44	O(2)−H(17B)	2.62
C(66)−H(66A)−O(6)	115.92	C(17)−H(17A)−O(3)	137.56
C(66)−H(66B)−O(7)	115.63	C(17)−H(17B)−O(2)	101.49

Ar(3), 2.67; H(33B)---Ar(2), 2.61 Å) are similar to the CH---arene contacts in $[Ca^{2+}(THF)_6][Me_3Si(fluorenyl)_2]\cdot C_6H_6$ (2.725–2.777 Å).[18] The third weak interaction in **3** is NCH_2−H---O hydrogen bonding between the NMe group and the OMe groups on Ar(2) and Ar(3) (Figure 1).[19] The O(3)---H(17A) distance (2.30 Å) is 0.4 Å shorter than the sum of the O and H van der Waals radii (2.72 Å), and the C(17)−H(17A)−O(3) angle (137.56°) is in the range typically observed for such interactions.[19] The O(2)---H(17B) distance is also short (2.62 Å), but the C(17)−H(17B)−O(2) angle (101.49°) is smaller than normally observed in H-bonded structures.[19] It is, of course, difficult to determine if these weak interactions *dictate* the arrangement of aryl groups in **3** or simply result from a sterically controlled arrangement of the aryl groups.

We also computed the gas phase structure of {PNP}NiBr$_2$ (**3**) by DFT. The calculated structure is very similar to that determined by X-ray diffraction (see Supporting Information). In particular, it shows the same orientation of the phenyl rings, with Ni**---**H(10,19) distances of 2.83 and 2.87 Å and OCH**---** (Ar centroid) distances of 2.83 and 2.86 Å. These close similarities between the computed gas phase structure and the experimentally determined solid state structure argue against crystal-packing forces directing the conformation of the PNP ligand.

Dynamic Properties of 3. The room-temperature ^{1}H, ^{13}C, and ^{31}P NMR spectra of **3** in CD_2Cl_2 display sharp signals consistent with a diamagnetic square-planar Ni species in solution. The room-temperature ^{1}H spectrum (Figure 2) contains one set of aryl resonances, one singlet for the methoxy groups (δ 3.45), and one singlet for the methyl groups (δ 2.30), indicating that the four aryl groups of the PNP ligand are equivalent on the NMR time scale. Upon lowering the temperature, all of these resonances broaden and split. The 165 K ^{1}H NMR spectrum (Figure 2) contains two partly resolved sets of resonances, consistent with the presence of two isomers, **3a** and **3b**, in a ca. 10:3 ratio. The spectrum of the major species **3a** is consistent with the structure observed for **3** in the solid state. Key resonances for **3a** include (i) two OCH_3 singlets of equal intensity (6H each), one in the normal range (δ 3.45) and the other ca. 0.5 ppm upfield from the normal range (δ 2.88), presumably due to anisotropic shielding resulting from the CH---π interaction noted above; (ii) two *ortho*-aryl resonances, one overlapped with the H_{meta} and H_{para} resonances at δ 7.39–6.73 and the other shifted significantly downfield to δ 8.92, presumably due to the CH---Ni interaction noted above,[20] and (iii) two H_{meta}, two H_{para}, and two Ar−Me resonances. The resonances for the minor isomer **3b** are mostly hidden by those of **3a**, but one OCH_3 resonance (δ 3.45) and one H_{ortho} resonance (δ ca. 8.3, br) can be identified for this species.[21] The structure of **3b** cannot be assigned from the limited data available, but presumably differs from that of **3a** in the conformation of the aryl rings.[22]

The existence of the two isomers **3a** and **3b** at low temperature was confirmed by ^{31}P NMR spectroscopy (Figure

(12) van der Waals radii: Ni: 1.63 Å; O: 1.52 Å; H 1.20 Å. See: Bondi, A. *J. Phys. Chem.* **1964**, *68*, 441.

(13) The data reported correspond to calculated H atom positions. These hydrogens were also located in the Fourier difference map, leading to similar distances: H(10)---Ni(1) = 2.84(3) Å, H(19)---Ni(1) = 2.86(3) Å, H(43)---Ni(2) = 2.96(3) Å, H(51)---Ni(2) = 2.86(3) Å.

(14) Yao, W.; Eisenstein, O.; Crabtree, R. H. *Inorg. Chim. Acta* **1997**, *254*, 105.

(15) Kitiachvili, K. D.; Mindiola, D. J.; Hillhouse, G. L. *J. Am. Chem. Soc.* **2004**, *126*, 10554.

(16) Brammer, L. *J. Chem. Soc., Dalton Trans.* **2003**, 3145.

(17) Ma, J. C.; Dougherty, D. A. *Chem. Rev.* **1997**, *97*, 1303.

(18) Harder, S.; Feil, F.; Repo, T. *Chem.−Eur. J.* **2002**, *8*, 1991.

(19) Desiraju, G. R. *Acc. Chem. Res.* **1996**, *29*, 441.

(20) The EXSY spectrum of **3** at 153 K in $CDCl_2F$−CD_2Cl_2 (1:6) shows a correlation between the two *ortho*-aryl protons at δ 8.96 and 6.97.

(21) The **3a/3b** ratio is estimated to be 10:3 from the integrated intensities of the OCH_3 resonances, and the intensities of the other (overlapped) resonances are consistent with this ratio. For example, the 12 aryl hydrogen resonances of **3b** overlap with 10 of the aryl hydrogen resonances of **3a** in the region δ 7.51–6.65 (total integration = I_2), while the two remaining aryl hydrogen resonances of **3a** are shifted downfield at δ 8.92 (I_1). The experimental value for the I_2/I_1 ratio of 7.3 corresponds well with the I_2/I_1 ratio of 7.5, expected for a 10:3 **3a/3b** ratio.

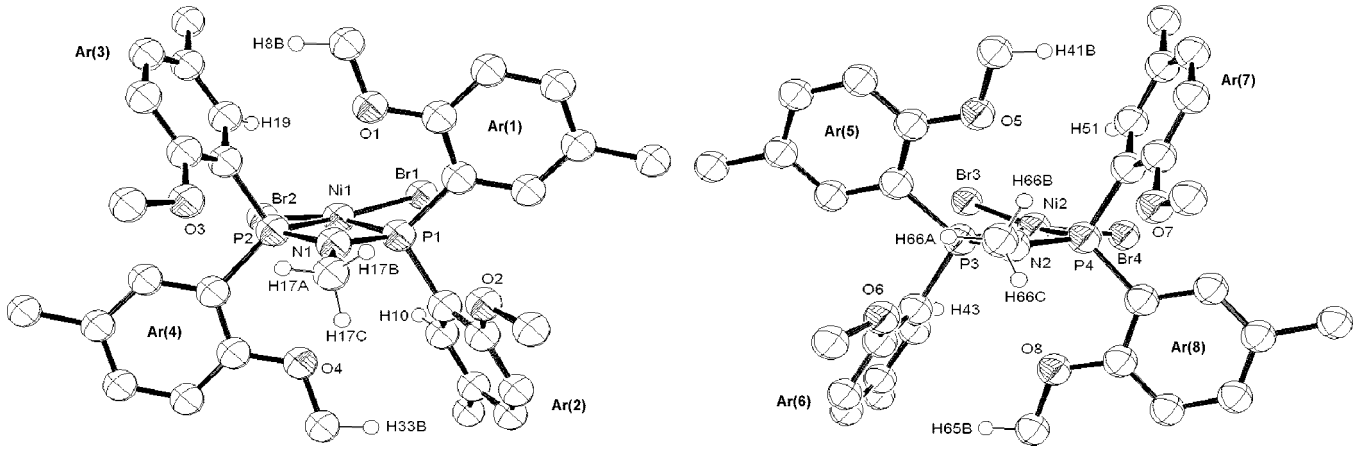

Figure 1. ORTEP views of the two independent molecules in the unit cell of {PNP}$NiBr_2$ (**3**). Hydrogen atoms have been omitted except H(33B), H(8B), H(19), H(17A), H(17B), H(17C), and H(10) for **Ni(1)** and H(41B), H(65B), H(51), (H43), H(66A), H(66B), and H(66C) for **Ni(2)**.

Table 3. Selected Torsion Angles α (deg) for the Two Independent Molecules (Ni(1) and Ni(2)) Found in {PNP}$NiBr_2$ (3)[a]

Ni(1)			Ni(2)		
Ni(1)−P(1)−C(1)−C(6)	Ar(1)	−58.63	Ni(2)−P(3)−C(39)−C(34)	Ar(5)	59.11
Ni(1)−P(1)−C(9)−C(14)−	Ar(2)	169.10	Ni(2)−P(3)−C(42)−C(47)	Ar(6)	−167.70
Ni(1)−P(2)−C(18)−C(23)	Ar(3)	165.51	Ni(2)−P(4)−C(50)−C(55)	Ar(7)	64.18
Ni(1)−P(2)−C(26)−C(31)	Ar(4)	−61.90	Ni(2)−P(4)−C(58)−C(63)	Ar(8)	−154.85

[a] The torsion angle is counted positive if the Ni−P−C(*ipso*P) angle is rotated clockwise vs the P−C(*ipso*P)−C(*ipso*O) angle.[39] Ar(*x*) refers to the numbering of the aryl rings in Figure 1.

3). The $^{31}P\{^1H\}$ spectrum consists of a sharp singlet (δ 39.1) at room temperature, which broadens and splits as the temperature is lowered. At 190 K, two resonances are observed at δ 39.1 and 38.1 in a ca. 10:2 ratio.[23,24] These ^1H and ^{31}P NMR line shape phenomena are all reversible upon lowering or increasing the temperature.

The overall structure and the weak interactions observed for **3** resemble those of other complexes that contain OMe-Ar-phosphine ligands. In particular, the solid state structures of Ni(*o*-MeO-dppp)X_2 (X = Cl or Br),[1c] Ni(*o*-MeO-dppe)I_2,[1d] and Ni(*o*-MeO-dpppol)Cl_2[1g] (see Chart 1 for ligand definitions) exhibit an edge/face arrangement of aryl groups without coordination of the methoxy group to Ni. The Ni coordination geometry in these complexes is square planar, with a similar tetrahedral distortion as observed in **3**. The dihedral angles between the X−Ni−X and P−Ni−P planes are 16.65° and 19.45° for Ni(*o*-MeO-dppp)X_2 (X = Cl, Br), 3.30° for Ni(*o*-MeO-dppe)I_2), and 11.50° for **Ni(1)** and 14.30° for **Ni(2)** in **3**. Also, the Ni---H distances in Ni(*o*-MeO-dppe)I_2 (2.79 and 2.78 Å) and Ni(*o*-MeO-dppe)X_2 (X = Cl, 2.87 Å; X = Br, 2.84 Å) are similar to those in **3** (2.84 and 2.83 Å in **Ni(1)**).

Synthesis and Structure of {PNP}$_2$Ni (4). The reaction of $Ni(cod)_2$ with 2 equiv of **2** in toluene at room temperature affords {PNP}$_2$Ni (**4**) in 61% yield as a red powder (eq 2). The solid state structure of **4** was determined by X-ray diffraction. Crystal data and selected bond lengths and angles are listed in Tables 1 and 4. Complex **4** adopts a distorted tetrahedral geometry (Figure 4). The main distortions are the acute P−Ni−P angles ((P(1)−Ni(1)−P(1_2) = 74.58(5)°, P(2)−Ni(1)−P(2_2) = 74.84(5)°). The Ni−P bond distances (2.166(1)−2.172(1) Å) are in the range reported for other Ni(0) complexes.[1b,6a,25] There are no close Ni---O contacts (Ni---O distances >4.2 Å) or Ni---H contacts (Ni---H distances >3 Å). Two interligand CH−π interactions involving the *o*-OMe hydrogen atoms H(26b) and H(26b_2) and the aryl rings C(11)−C(16) and C(11_1)−C(16_1) are observed in **4**. The corresponding C−H---$arene_{centroid}$ distances (H(26b)---(centroid C(11)−C(16)), 2.64 Å) are similar to those in **3**. One methyl hydrogen on N(2) is hydrogen-bonded to an oxygen atom (O(4)---H(2a), 2.59 Å; C(2)−H(2a)−O(4), 147.5°).[19]

Dynamic Properties of 4. The ^1H NMR spectrum of **4** at high temperature (376 K) contains one set of aryl resonances, one OMe resonance (δ 3.45), one N−Me resonance (δ 2.58), and one Me−aryl resonance (δ 2.13), indicating that all of the PNP aryl rings are equivalent on the NMR time scale. Upon lowering the temperature, the aryl, OMe, and Me−aryl reso-

(22) (a) The barriers determined from the coalescence of the H_{ortho} resonances, OMe resonances, and Ar−Me resonances of the major isomer **3a** in the ^1H NMR spectra are equal ($\Delta G^{\ddagger}$ = 9.2(2) kcal/mol; *vide infra*), which suggests that these coalescences result from the same fluxional process. Note, however, that the calculated barriers do not take into account the effect of the possible **3a/3b** exchange. (b) Exchange barriers $\Delta G^{\ddagger}$ were determined from the coalescence of the H_{ortho} resonances (T_{coal} = 212 K), OMe resonances (T_{coal} = 205 K), and Ar−Me (T_{coal} = 200 K) resonances of **3a**, using the following equations for an equally populated, two-site exchange: $\Delta G^{\ddagger} = 4.576T_c[10.319 + \log(T_c/k_c)]$, where T_c is the coalescence temperature and k_c is the exchange rate constant at coalescence, which is given by $k_c = \pi[(\Delta\nu_{AB}^2 + 6J_{AB}^2]^{1/2}/2^{1/2}$.[b−d] The uncertainties in ΔG_{coal} were estimated assuming ±2% uncertainty in the chemical shifts and coalescence temperature. (c) Alexander, S. *J. Chem. Phys.* **1962**, *37*, 967. (d) Kurland, R. J.; Rubin, M. B.; Wise, W. B. *J. Chem. Phys.* **1964**, *40*, 2426. (e) Kost, D.; Zeichner, A. *Tetrahedron Lett.* **1974**, 4533.

(23) The difference in the **3a/3b** ratio estimated by ^1H and ^{31}P NMR is primarily due to the uncertainty in the latter measurement, which is imprecise due to the broadness of the resonance for the minor species **3b**.

(24) The barrier for **3a/3b** exchange was estimated to be $\Delta G_{coal}^{\ddagger}$ = 10.9(3) kcal mol^{-1} at T_{coal} = 206 K from the ^{31}P NMR spectra, which were analyzed as an unequally populated, two-site exchange system, using the method of Shanan-Atidi, H.; Bar-Eli, K. H. *J. Phys. Chem.* **1970**, *74*, 961. The uncertainty in $\Delta G_{coal}^{\ddagger}$ was estimated assuming ±2% uncertainty in the chemical shifts and coalescence temperature, and relative populations in the range 10:3 to 10:2.

(25) (a) Bennett, B. L.; White, S.; Hodges, B.; Rodgers, D.; Lau, A.; Roddick, D. M. *J. Organomet. Chem.* **2003**, *679*, 65. (b) Edelbach, B. L.; Lachicotte, R. J.; Jones, W. D. *Organometallics* **1999**, *18*, 4040. (c) Shimada, S.; Rao, M. L. N.; Hayashi, T.; Tanaka, M. *Angew. Chem., Int. Ed.* **2001**, *40*, 213.

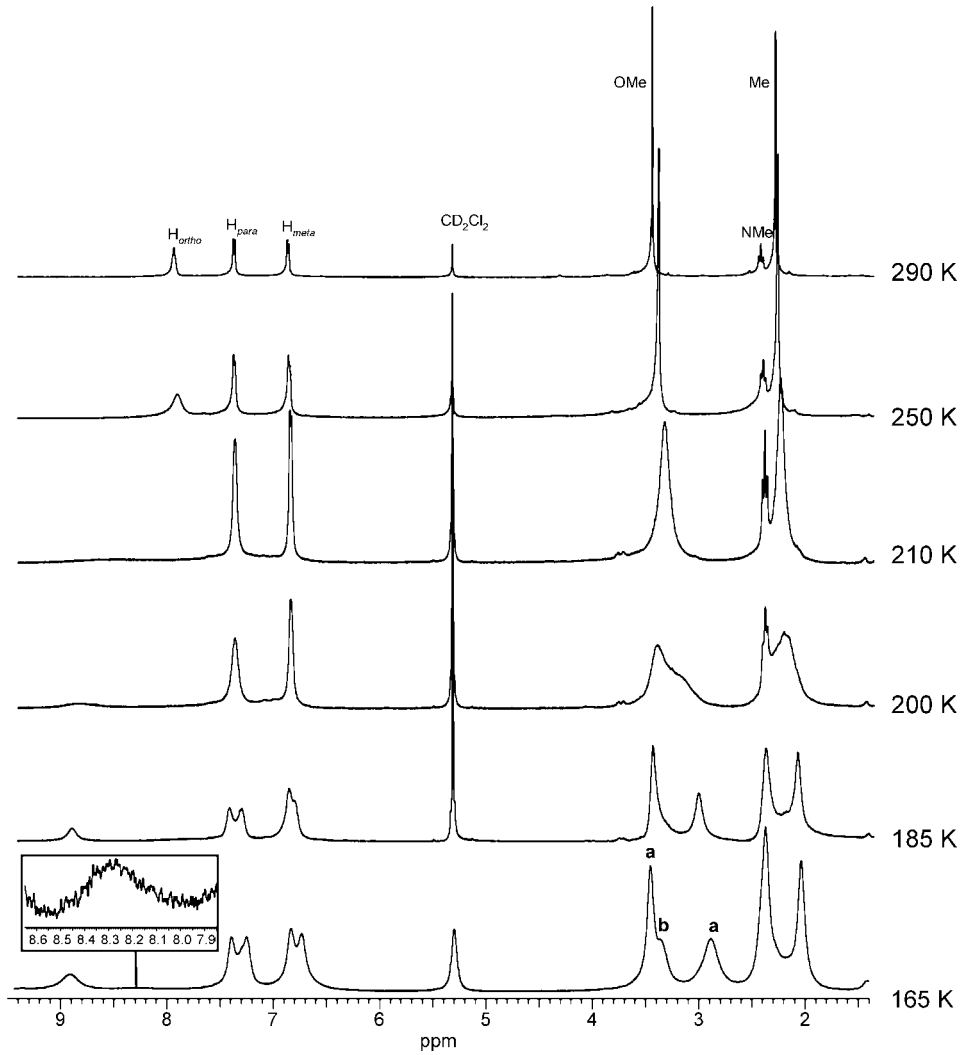

Figure 2. Variable-temperature ^{1}H NMR spectra (500 MHz, CD_2Cl_2) of {PNP}$NiBr_2$ (**3**). The markers **a** and **b** in the 165 K spectrum identify the OMe resonances of the major isomer **3a** and the minor isomer **3b**, respectively.

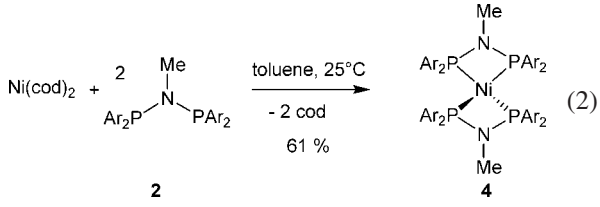

2 **4** (2)

nances broaden and split into two sets of resonances in a 1:1 intensity ratio (assigned by 2D NMR and labeled **a** and **b** in Figure 5), and the N−Me resonance shifts slightly but does not split. In the low-temperature spectrum, one H_{ortho} resonance corresponding to four *ortho* hydrogens is shifted to low field (δ 8.73), similar to what was observed for **3**. These results are consistent with a C_2-symmetric static structure of **4** that is similar to that observed in the solid state and with rapid exchange of the aryl ring environments via rotation around the P−Ar bonds. The exchange barrier $\Delta G^{\ddagger} = 14.1(3)$ kcal mol^{-1} was determined from the coalescence of the H_{ortho} resonances (T_{coal} = ca. 325 K) and the OMe resonances (T_{coal} = 290 K).[22]

Synthesis of {PNP}Ni(cod) (5). The reaction of $Ni(cod)_2$ with 1 equiv of **2** in toluene or benzene affords {PNP}Ni(cod) (**5**) in 90% yield as a brown powder (eq 3). NMR monitoring experiments show that this reaction occurs by a multistep mechanism. The ^{1}H NMR spectrum of a 1:1 mixture of **2** and $Ni(cod)_2$ in benzene-d_6 after 5 min at 25 °C contained resonances for bis(ligand) complex **4** and 50% of the starting $Ni(cod)_2$, but no resonances for free ligand **2**. Over 2 h at room temperature, the resonances for **4** and $Ni(cod)_2$ disappeared, while the resonances for **5** appeared. Similarly, the ^{31}P{^{1}H} NMR spectrum of a 1:1 $Ni(cod)_2$/**2** mixture recorded after 5 min contained a major resonance for **4** and a minor resonance for **5** as shown in Figure 6. Over 2 h, the resonances for **4** disappeared while the resonances for **5** grew in.

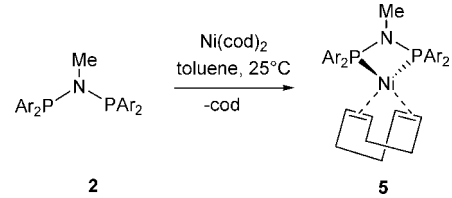

2 **5** (3)

These observations show that the formation of **5** proceeds as shown in Scheme 2. $Ni(cod)_2$ reacts with **2** to give **5**, but **5** reacts rapidly with a second equivalent of **2** to yield **4**. Subsequent slow comproportionation of **4** and $Ni(cod)_2$, probably by dissociation of one arm of a PNP ligand of **4** and one arm of a cod ligand of **5**, yields **5** (Scheme 2).

Complex **5** is stable in the solid state at −30 °C but decomposes to **4** and Ni^0 at room temperature in aromatic solvents. ^{31}P{^{1}H} NMR monitoring of a freshly prepared

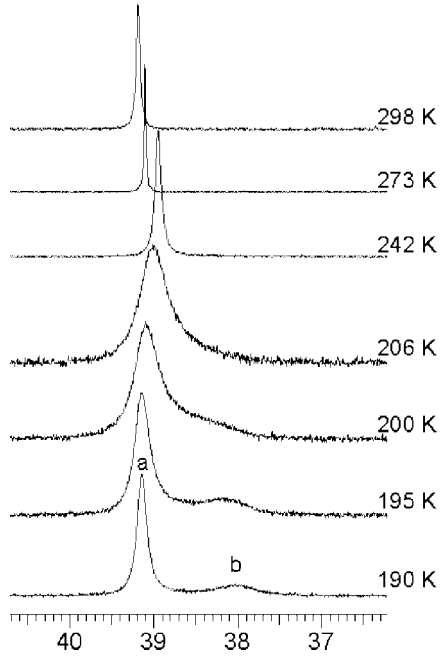

Figure 3. Variable-temperature $^{31}P\{^1H\}$ NMR spectra (200 MHz, CD_2Cl_2) of {PNP}NiBr$_2$ (**3**). The markers **a** and **b** stand for the resonances of the major isomer **3a** and the minor isomer **3b** respectively.

solution of **5** (δ 72.9) in benzene-d_6 (Figure 7) revealed that the latter complex is almost completely consumed with concomitant formation of **4** (δ 79.9) after 3 days. These results suggest that **5** slowly decomposes to Ni^0 and free **2**, which further reacts with remaining **5** to yield **4** (Scheme 3).

Protonation of 5. The reaction of **5** with 1 equiv of $[H(OEt_2)_2][B(C_6F_5)_4]$ at low temperature produces a new species formulated as {PNP}Ni(codH)$^+$ (**6**, $B(C_6F_5)_4^-$ salt, eq 4). ^1H NMR data for **6** in toluene-d_8, CD_2Cl_2, and chlorobenzene-d_5 at different temperatures are difficult to interpret due to (i) a systematic broadening of the signals, possibly caused by the presence of minor paramagnetic coproducts, and (ii) the probable presence of several isomers. Earlier, Keim showed that the reaction of Ni(cod)$_2$ with $Ph_2PCH_2CO_2H$ yields (C_8H_{13})-$(Ph_2PCH_2CO_2)$Ni, which exists as a mixture of η^3-allyl and κ^2-alkyl-4-ene species.[26] However, the ESI-MS spectrum of **6** confirmed that the {PNP}Ni(codH)$^+$ cation is the major cation present.

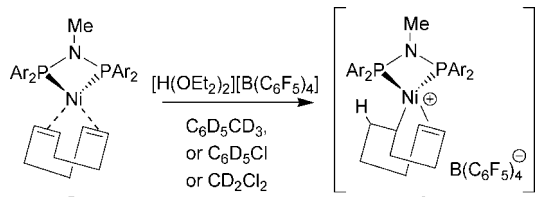

(4)

Ethylene Polymerization Studies. Complexes **3** and **5** were briefly investigated in ethylene polymerization using the activation protocols in Scheme 4.

The reaction of **3** with MAO (200 equiv), which may be expected to generate a {PNP}NiMe$^+$ species (Scheme 4(i)),[27] resulted in an immediate color change from bright red to pale yellow. Upon pressurization with ethylene, very low ethylene consumption (ca. 5–10 (mol C_2H_4) (mol Ni)$^{-1}$ h^{-1} over 30 min) and significant formation of Ni^0 were observed. Hydrolytic workup did not afford any polymer, but GC analysis of the volatiles revealed the presence of small amounts of butenes, hexenes, and higher α-olefins.

Table 4. Selected Bond Distances (Å) and Angles (deg) for {PNP}$_2$Ni (4)

Ni(1)−P(1)	2.1664 (10)	P(1)−Ni(1)−P(1_2)	74.58 (5)
Ni(1)−P(2)	2.1721 (10)	P(2)−Ni(1)−P(2_2)	74.84 (5)
P(1)−N(1)	1.704 (3)	P(1)−Ni(1)−P(2)	125.84 (3)
P(2)−N(2)	1.704 (3)	P(1)−Ni(1)−P(2_2)	132.70 (3)

The ternary system Ni(cod)$_2$/**2**/$[H(OEt_2)_2][B(3,5\text{-}(CF_3)_2C_6H_3)_4]$ (Scheme 4(ii)) does produce polyethylene with moderate activity (entries 1–4). However, the catalyst performance is very sensitive to the activation protocol. For entries 1–4, Ni(cod)$_2$, **2**, and $[H(OEt_2)_2][B(3,5\text{-}(CF_3)_2C_6H_3)_4]$ were reacted for 5 min at 0 °C in toluene and then for 5 min at the polymerization temperature (20–80 °C) prior to addition of ethylene. However, when the activation was conducted at 0 °C only (5–60 min), low irreproducible polymerization activities were observed. These differences are ascribed to slow rate and indirect mechanism of formation of **5** from Ni(cod)$_2$ and **2** (Scheme 3), the possible reaction of $H(OEt_2)_2^+$ with **2**, **4**, or other species,[28] and the decomposition of **5** to **2** and Ni^0. These observations show that simple precursor/ligand/activator combinations do not necessarily lead to the expected species in this system.

To avoid complications related to the *in situ* generation of **5** in the ternary catalyst, preformed **5** was activated by $[H(OEt_2)_2][B(C_6F_5)_4]$ under ethylene pressure, to initially generate cationic species **6** (Scheme 4(iii)). This "binary" catalyst exhibits reproducible activity (entries 5–7) and produces moderately branched[29] (7–15 branches/1000C), low molecular weight PE, with mostly vinyl and 2-olefin unsaturated chain ends. Methyl and ethyl branches predominate, and only small amounts of propyl and longer branches were observed by ^{13}C NMR.[30,31] These results are consistent with chain walking competing poorly with chain growth under these conditions.

Wass' alkyl-substituted-PNP Ni catalysts, generated *in situ* from $[Ni(cod)_2]/[H(Et_2O)_2][B(3,5\text{-}(CF_3)_2C_6H_3)_4]/\{(2\text{-R-}C_6H_4)_2\text{-}P\}_2NMe$ (R = Me, Et), showed similar activities (60–100 (kg PE) mol^{-1} h^{-1}, 25 °C, 1 atm ethylene) and afforded materials similar to those produced by **5**/$[H(OEt_2)_2][B(C_6F_5)_4]$, with low molecular weights (R = Me: M_n = 4000 g mol^{-1}, M_w/M_n = 2.2; R = Et: M_n = 9000 g mol^{-1}, M_w/M_n = 2.5) and moderate branching (8–11 branches/1000C, predominantly methyl branches).[8,32]

Computational Studies of {PNP}Ni(alkyl)$^+$ Species. The gas phase structures of {PNP}Ni(*n*-propyl)$^+$ and {PNP}Ni(*n*-propyl)$(C_2H_4)^+$ were computed by DFT (see Supporting Information). The latter species is a model for the {PNP}Ni(codH)$^+$ cation in **6** and for the presumed active propagating species in ethylene polymerization. For {PNP}Ni(*n*-propyl)$^+$, the structure with a β-agostic *n*-propyl ligand was found to be 11.1 kcal

(26) Peuckert, M.; Keim, W. *Organometallics* **1983**, *2*, 594.

(27) (a) Johnson, L. K.; Killian, C. M.; Brookhart, M. *J. Am. Chem. Soc.* **1995**, *117*, 6414. (b) Killian, C. M.; Johnson, L. K.; Brookhart, M. *Organometallics* **1997**, *16*, 2005. (c) Svejda, S. A.; Brookhart, M. *Organometallics* **1999**, *18*, 65. (d) Gates, D. P.; Svejda, S. A.; Onate, E.; Killian, C. M.; Johnson, L. K.; White, P. S.; Brookhart, M. *Macromolecules* **2000**, *33*, 2320. (e) Leatherman, M. D.; Svejda, S. A.; Johnson, L. K.; Brookhart, M. *J. Am. Chem. Soc.* **2003**, *125*, 3068.

(28) No polymerization activity was observed for **4**/$[H(OEt_2)_2][B(3,5\text{-}(CF_3)_2C_6H_3)_4]$ (1:1) (20 °C, 5 atm ethylene, for 20 min).

(29) Gottfried, A. C.; Brookhart, M. *Macromolecules* **2003**, *36*, 3085.

(30) Galland, G. B.; de Souza, R. F.; Mauler, R. S.; Nunes, F. F. *Macromolecules* **1999**, *32*, 1620.

(31) Distribution of branches, as evaluated by $^{13}C\{^1H\}$ NMR (Table 5, entry 7): Me, 55%; Et, 29%; Pr, <5%; Bu and higher, 16%.

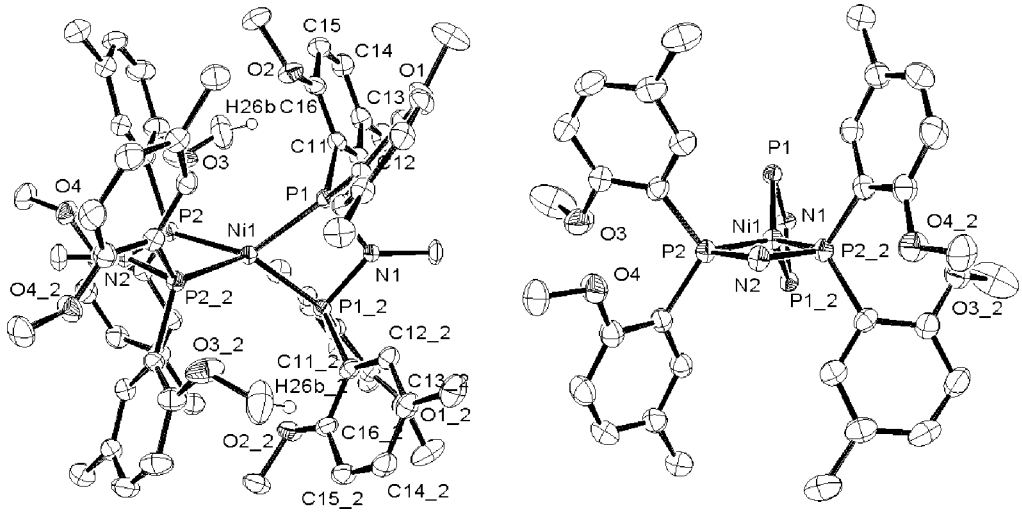

Figure 4. ORTEP views of {PNP}$_2$Ni (**4**). Left: View of the full molecule, with hydrogen atoms omitted, except H(26b). Right: View showing the orientation of the aryl rings of one PNP ligand along the N(2)−Ni(1)−N(1) axis; the aryl rings on P(1) and P(1_2) and all hydrogens have been omitted.

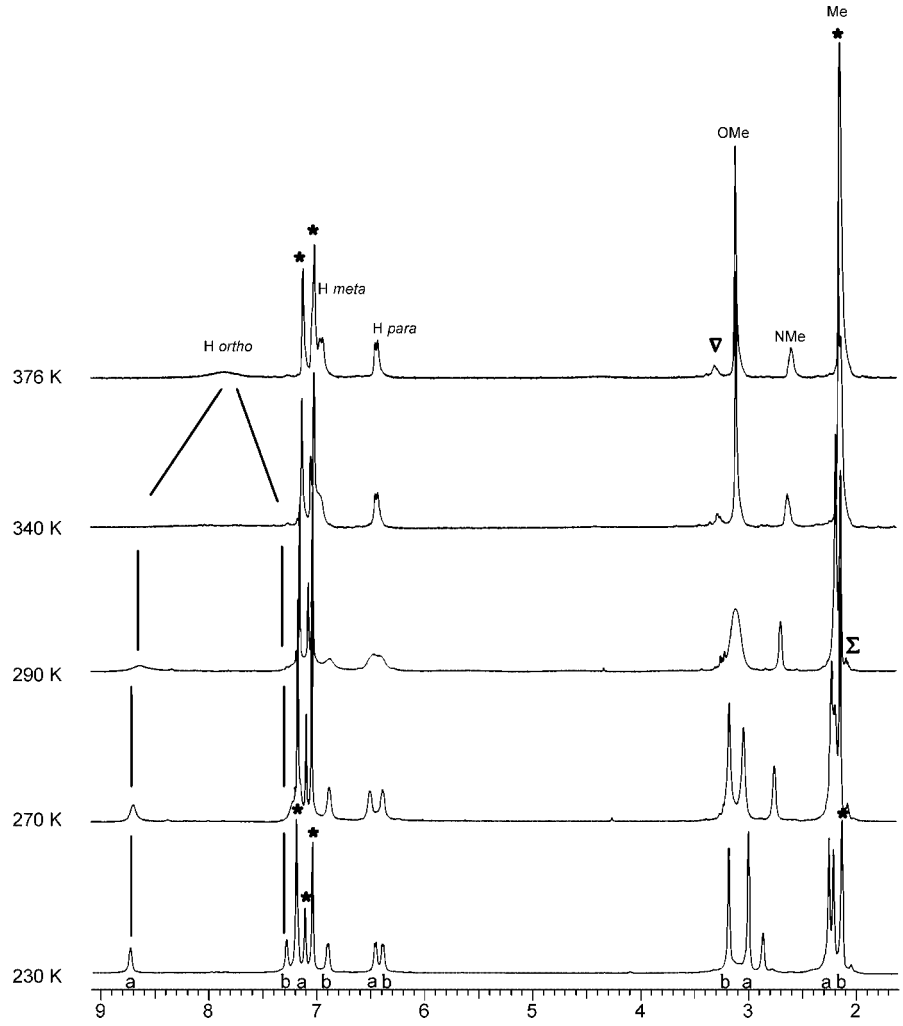

Figure 5. Variable-temperature ^{1}H NMR spectra (500 MHz, toluene-d_8) of {PNP}$_2$Ni (**4**). The markers **a** and **b** denote resonances for the two inequivalent aryl groups. The markers *, Σ, and ▽ denote resonances for toluene, PhC*H*D$_2$, and Et$_2$O, respectively.

mol^{-1} more stable than the corresponding α-agostic structure. No agostic interactions were found in {PNP}Ni(*n*-propyl)-$(C_2H_4)^+$. The conformation of the PNP ligands in the optimized structures of *β*-agostic {PNP}Ni(*n*-propyl)$^+$ and {PNP}Ni(*n*-propyl)$(C_2H_4)^+$ are both very similar to that observed for **3** by X-ray diffraction and computed by DFT, *vide supra*. All three species exhibit a similar edge-face arrangement of the aryl rings, weak CH---Ni interactions involving the *ortho* aryl hydrogens, and weak CH−*π* interactions involving the OMe hydrogens and the aryl rings.[33] Thus, even in an electron-deficient species such

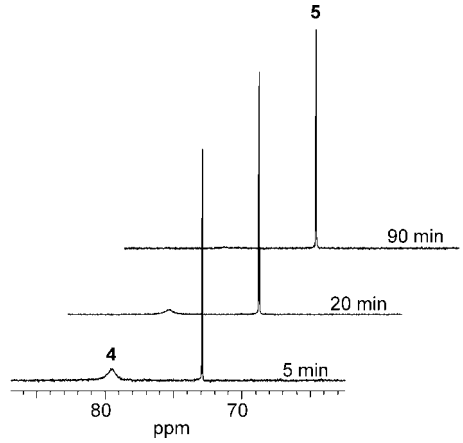

Figure 6. $^{31}P\{^{1}H\}$ NMR monitoring (200 MHz) of the 1:1 reaction of PNP (**2**) with $Ni(cod)_2$ in benzene-d_6 at room temperature. $\{PNP\}_2Ni$ (**4**): δ 79.9; {PNP}Ni(cod) (**5**): δ 72.9.

Scheme 2

$Ni(cod)_2$ + **2** $\xrightarrow[-cod]{}$ {PNP}Ni(cod) (**5**)

5 + **2** $\xrightarrow[-cod]{fast}$ $\{PNP\}_2Ni$ (**4**)

$Ni(cod)_2$ + **4** $\xrightarrow[-cod]{slow}$ 2 {PNP}Ni(cod) (**5**)

as $\{PNP\}Ni(n\text{-propyl})^+$, coordination of the *ortho*-OMe groups to Ni is not favored.

Conclusion

The reaction of $(dme)NiBr_2$ with $\{(2\text{-OMe-4-Me-Ph})_2P\}_2NMe$ (**2**, PNP) yields $\{PNP\}NiBr_2$ (**3**). The reaction of $Ni(cod)_2$ with **2** yields {PNP}Ni(cod) (**5**). This reaction is not straightforward but proceeds via initial formation of $\{PNP\}_2Ni$ (**4**), followed by slow comproportionation with $Ni(cod)_2$. X-ray crystallographic analyses of **3** and **4**, supported by DFT studies for **3**, show that the methoxy groups do not coordinate to Ni but reveal the presence of weak CH---Ni interactions involving the *ortho* aryl hydrogens, and weak CH$-\pi$ interactions involving the OMe hydrogens and the aryl rings. The reaction of**5** with $[H(OEt_2)_2][B(3,5\text{-}(CF_3)_2C_6H_3)_4]$ or $[H(OEt_2)_2][B(C_6F_5)_4]$ generates a cationic species formulated as $\{PNP\}Ni(codH)^+$ (**6**) based on ESI-MS data. Cation **6**, generated *in situ* from **5** and $[H(OEt_2)_2][B(C_6F_5)_4]$, polymerizes ethylene with reproducible activity to low molecular weight, moderately branched polymer. In contrast, the performance of the ternary system $Ni(cod)_2$/**2**/$[H(OEt_2)_2][B(3,5\text{-}(CF_3)_2C_6H_3)_4]$ is very sensitive to the activation protocol, probably as a result of the slow rate and indirect mechanism of formation of **5** from $Ni(cod)_2$ and **2**. DFT studies show that the PNP ligands in the model species $\{PNP\}Ni(n\text{-propyl})^+$ (β-agostic isomer) and $\{PNP\}Ni(n\text{-propyl})(C_2H_4)^+$ adopt conformations that are very similar to that in **3**, with the same CH---Ni and OCH**---**π interactions and no significant interaction between the *ortho*-methoxy groups and the Ni centers.

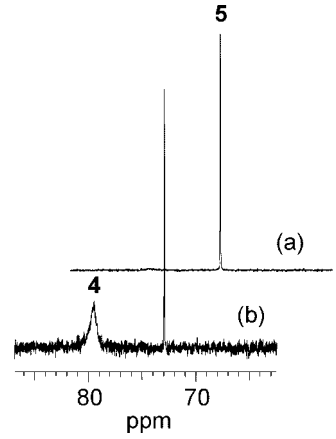

Figure 7. $^{31}P\{^{1}H\}$ NMR spectrum (200 MHz, benzene-d_6, 25 °C) of (a) a freshly prepared solution of **5**; (b) the same solution after 72 h at 25 °C.

Scheme 3

{PNP}Ni(cod) (**5**) $\longrightarrow$ PNP (**2**) + Ni° + cod

{PNP}Ni(cod) (**5**) $\rightleftharpoons$ $\{PNP\}_2Ni$ (**4**) (**2**)

Scheme 4

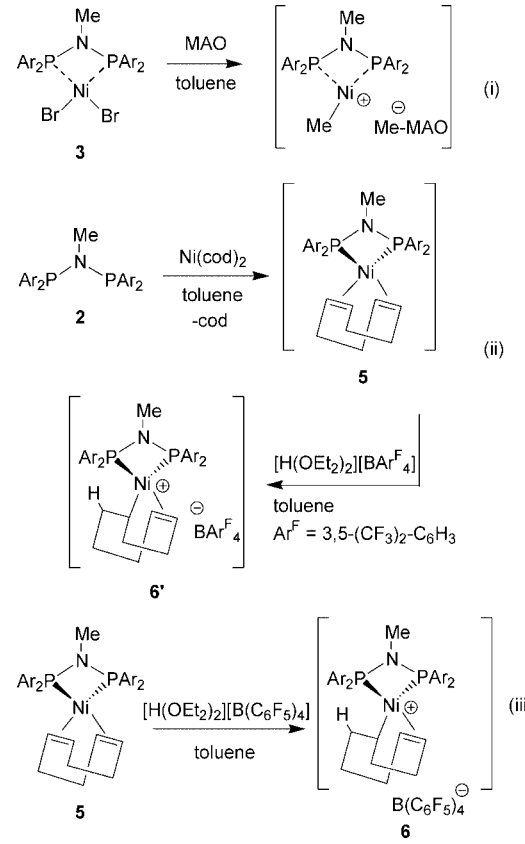

Experimental Section

General Considerations. All manipulations were performed under a purified argon or nitrogen atmosphere using standard high-vacuum or Schlenk techniques or in a glovebox. Solvents (toluene, pentane, THF) were freshly distilled from Na/K alloy under nitrogen and degassed thoroughly by freeze–thaw−vacuum cycles prior to use. Methylene chloride-d_2 and chloroform-d_1 were distilled over CaH_2/P_2O_5 and degassed prior to use. Toluene-d_8 and benzene-d_6

(32) Cooley, N. A.; Green, S. M.; Wass, D. F. *Organometallics* **2001**, *20*, 4769.

(33) The computed CH---Ni distances are Ni---H(10, 19) = 2.85, 2.87 Å for {PNP}Ni(*n*-propyl)+ and 2.80, 2.82 Å for {PNP}Ni(*n*-propyl)-$(C_2H_4)^+$. The computed OCH---(Ar centroid) distances are 2.76, 2.79 Å for $\{PNP\}Ni(n\text{-propyl})^+$ and 2.73, 2.78 Å for $\{PNP\}Ni(n\text{-propyl})(C_2H_4)^+$.

were freshly distilled from Na/K or Na/benzophenone under argon and degassed prior to use. 2-Bromo-4-methylanisole (Acros) was dried over molecular sieves (3 Å) and freeze–pump–thaw degassed three times before use. PBr_3 (Acros) was vacuum distilled. Methylamine (2.0 M solution in THF, Acros) was used as received. $NiBr_2$(dme), $Ni(cod)_2$, and MeMgBr (1.0 M solution in Et_2O) were purchased from Aldrich and used without purification. MAO (30 wt % solution in toluene, Albermarle) and $[HNMe_2Ph][B(C_6F_5)_4]$ (Boulder Chemicals) were used as received. $[H(OEt_2)_2][B(3,5\text{-}(CF_3)_2C_6H_3)]_4$ and $[H(OEt_2)_2][B(C_6F_5)_4]$ were synthesized by published methods.[34]

NMR spectra were recorded on Bruker AC-300 and AM-500 spectrometers in Teflon-valve NMR tubes at ambient probe temperature (23 °C) unless otherwise indicated. ^1H and ^{13}C chemical shifts are reported vs $SiMe_4$ and were determined by reference to the residual solvent peaks. NMR assignments were made from $^1H-^1H$ COSY, $^1H-^{13}C$ HMQC, and HMBC NMR experiments. All coupling constants are given in hertz.

Electron impact high-resolution mass spectra (EI-HRMS) of organic compounds were recorded on a high-resolution MS/MS spectrometer Micromass ZABSpecTOF. Electrospray mass spectra (ESI-MS) were recorded on freshly prepared samples (dichloromethane solutions) using an Agilent 1100 LC-MSD spectrometer incorporating a quadrupole mass filter with a *m*/*z* range of 0–3000.

Elemental analyses were performed by the Microanalytical Laboratory at the Institute of Chemistry of Rennes and are the average of two independent determinations. Gel permeation chromatography (GPC) was performed on a Polymer Laboratories PL-GPC 220 instrument using 1,2,4-trichlorobenzene solvent (stabilized with 125 ppm BHT) at 150 °C. A set of three PLgel 10 μm Mixed-B or Mixed-B LS columns was used. Samples were prepared at 160 °C. Polyethylene molecular weights were determined vs polystyrene standards and are reported relative to polyethylene standards, as calculated by the universal calibration method using Mark–Houwink parameters ($K = 1.75 \times 10^{-2}$ cm^3/g, $\alpha = 0.67$ for PS, $K = 5.9 \times 10^{-2}$ cm^3/g, $\alpha = 0.69$ for PE).[35] DSC measurements were performed on a TA Instruments DSC 2920 differential scanning calorimeter. Samples (2–8 mg in Al pans) were first annealed by heating from 20 to 160 °C at 20 °C/min, cooled to −20 at 20 °C/min, and then analyzed while being heated to 160 °C at 20 °C/min.

(2-Methoxy-5-methylphenyl)$_2$PBr (1). 2-Bromo-4-methylanisole (5.40 g, 0.027 mol) was added dropwise to a suspension of magnesium powder (1.30 g, 0.053 mol) in THF (100 mL). The mixture was stirred 2 h at room temperature, filtered, and cannula-transferred to a solution of PBr_3 (1.19 mL, 0.013 mol) in THF (300 mL). The mixture was stirred at room temperature for 30 min. The solvent was removed under vacuum, and crude material was extracted with toluene (3 × 100 mL). The combined extracts were filtered through a D_3 frit with a Celite pad, and the filtrate was concentrated to dryness under vacuum. The product was isolated as a white solid by repeated washing with pentane (3 × 20 mL) and dried under vacuum (3.20 g, 74%). ^1H NMR (CD_2Cl_2, 500 MHz): δ 7.22 (d, $^3J_{PH} = 9.2$, 2H, H_{ortho}), 6.83 (d, $^3J_{HH} = 5.5$, 2H, H_{para}), 6.83 (d, $^3J_{HH} = 5.5$, 2H, H_{meta}), 3.79 (s, 6H, OMe), 2.25 (s, 6H, Me). $^{13}C\{^1H\}$ NMR ($CDCl_3$, 75 MHz) (most of the J_{C-P} coupling constants could not be determined accurately due to the broadening of signals): δ 159.1 (d, $^2J_{CP} = 20$, C-6), 133.9 (br, C-2), 132.6 (br, C-3), 130.5 (br, C-4)), 112.7 (br, C-1), 110.7 (br, C-5), 56.2 (OMe), 20.6 (Me). $^{31}P\{^1H\}$ (CD_2Cl_2, 202 MHz): δ 63.5. EI-HRMS (*m*/*z*): $[M]^+$ ($C_{16}H_{18}O_2{}^{79}BrP$) calcd 352.02278; found 352.02222.

(2-OMe-4-Me-Ph)$_2$PNMeP(2-OMe-4-Me-Ph)$_2$ (PNP, 2). A solution of **1** (2.63 g, 7.44 mmol) in THF (50 mL) at room temperature was prepared, and NEt_3 (6.00 mL, 82 mmol) and then NH_2Me (1.86 mL of a 2.0 M solution in THF) were added. The resulting white suspension was stirred for 12 h at room temperature and decanted. The liquid phase was separated from solid residues by cannula filtration, and the volatiles were removed under vacuum. The residue was extracted with benzene (5 × 50 mL) and filtrated through a D_3 frit with a Celite pad. The filtrate was concentrated to dryness under vacuum. The product was isolated as a pure white solid by washing with pentane (3 × 20 mL) and dried under vacuum (1.51 g, 70%). ^1H NMR ($CDCl_3$, 300 MHz): δ 7.10 (dd, $^3J_{HH} = 8.3$, $^4J_{PH} = 2.0$, 4H, H_{meta}), 6.87 (dd, $^3J_{PH} = 4.8$, $^4J_{HH} = 2.0$, 4H, H_{ortho}), 6.76 (ddd, $^3J_{HH} = 8.3$, $^4J_{HH} = 2.3$, $^5J_{PH} = 2.3$, 4H, H_{para}), 3.55 (s, 12H, OMe), 2.44 (t, $^3J_{PH} = 2.9$, 3H, NMe), 2.19 (s, 12H, Me). ^{13}C NMR (CD_2Cl_2, 125 MHz): δ 158.8 (m br, C-6), 133.6 (dm, $^1J_{CH} = 157$, C-2), 129.3 (dm, $^1J_{CH} = 155$, C-4), 129.3 (q, $^2J_{CH} = 7$, C-3), 126.8 (m br, C-1), 110.4 (dd, $^1J_{CH} = 159$, $^3J_{CP} = 7.9$, C-5), 55.4 (q, $^1J_{CH} = 143$, OMe), 33.3 (q, $^1J_{CH} = 143$, NMe), 20.8 (qt, $^1J_{CH} = 127$, $^3J_{CH} = 5$, Me). $^{31}P\{^1H\}$ (CD_2Cl_2, 202 MHz): δ 52.3. EI-HRMS (*m*/*z*): $[M]^+$ ($C_{33}H_{39}NO_4P_2$) calcd 575.2354, found 575.2374, $[M - OMe]^+$ ($C_{32}H_{36}NO_3P_2$) calcd 544.2170, found 544.2141.

{PNP}NiBr$_2$ (3). A Schlenk flask was charged with **2** (0.241 g, 0.42 mmol) $NiBr_2$(DME) (0.129 g, 0.42 mmol), and dichloromethane (5 mL) at room temperature. A deep purple solution formed. The mixture was stirred overnight. The solvent was reduced to one-third under vacuum. The mixture was kept at −80 °C overnight, and large purple crystals formed. The crystals were collected by filtration, washed with toluene, and dried under vacuum (0.21 g, 75%). Crystals of {PNP}$NiBr_2 \cdot (1.5\ CH_2Cl_2)$ suitable for single-crystal X-ray diffraction analysis were obtained from a saturated solution of **3** in a 6:4 CH_2Cl_2−pentane solution at −80 °C. Anal. Calcd for $C_{34.5}H_{42}Br_2Cl_3NNiO_4P_2$ ($\mathbf{3} \cdot (1.5CH_2Cl_2)$): C, 44.97; H, 4.59; N, 1.52. Found: C, 45.12; H, 4.63; N, 1.56. ^1H NMR (CD_2Cl_2, 500 MHz, 298 K): δ 7.91 (m, 4H, H_{ortho}), 7.35 (d, $^3J_{HH} = 8.3$, 4H H_{para}), 6.85 (d, $^3J_{HH} = 8.3$, 4H, H_{meta}), 3.45 (s, 12H, OMe), 2.44 (t, $^3J_{PH} = 11.0$, 3H, NMe), 2.30 (s, 12H, Me). ^{13}C NMR (CD_2Cl_2, 125 MHz): δ 164.7 (br m, C-6), 141.4 (d, $^1J_{CH} = 161$, C-2), 139.0 (d, $^1J_{CH} = 159$, C-4), 134.6 (m, C-3), 120.7 (m br, C-1), 114.65 (d, $^1J_{CH} = 159$, C-5), 55.4 (q, $^1J_{CH} = 144$, OMe), 34.4 (q, $^1J_{CH} = 139$, NMe), 18.7 (q, $^1J_{CH} = 122$, Me). $^{31}P\{^1H\}$ NMR (CD_2Cl_2, 202 MHz): δ 39.4. At 165 K two sets of signals were observed in the ^1H and ^{31}P NMR spectra, consistent with the existence of two isomers of **3** in the ratio 10:3.

Major isomer (3a). ^1H NMR (CD_2Cl_2, 500 MHz, 165 K): δ 8.92 (m, br, 2H, H_{ortho}), 6.73–7.39 (m, br, 2H, H_{ortho}, 4H, H_{meta}, 4H, H_{para}), 3.42 (s, br, 6H, OMe), 2.88 (s, br, 6H, OMe), 2.37 (s, 6H, Me), 2.03 (s, 6H, Me); the NCH_3 resonance overlaps with others broad signals. $^{13}C\{^1H\}$ NMR (CD_2Cl_2, 125 MHz, 165 K): δ 158.5 (m br, C-6), 157.7 (m br, C-6), 140.2 (m br, C-2), 134.9 (m br, C-4), 134.4 (m br, C-4),130.4 (m br, C-3), 129.1 (m br, C-3), 115.9 (m br, C-1), 115.1 (m br, C-1), 111.0 (m br, C-5), 110.0 (m br, C-5), 55.5 (OMe), 36.3 (s br, NMe), 20.6 (Me), 20.4 (Me). $^{31}P\{^1H\}$ (CD_2Cl_2, 202 MHz, 165 K): δ 39.1 (br).

Minor isomer (3b). ^1H NMR (CD_2Cl_2, 500 MHz, 165 K): δ 6.73–7.39 (m, br, 12H, H_{ortho}, H_{meta}, and H_{para}), 3.45 (s, br, 12H, OMe), 2.37 (s, 12H, Me), the NCH_3 resonance overlaps with others broad signals. $^{31}P\{^1H\}$ NMR (CD_2Cl_2, 202 MHz, 165 K): δ 38.1 (br). HRMS (ESI, *m*/*z*): $[M - Br]^+$ ($C_{33}H_{39}NO_4{}^{79}BrP_2{}^{58}Ni$) calcd 712.0891, found 712.0898.

{PNP}$_2$Ni (4). A Schlenk flask was charged with **2** (0.200 g, 0.347 mmol) and $Ni(cod)_2$ (0.047 g, 0.173 mmol). Precooled toluene (−30 °C) was added by cannula at −30 °C, and the mixture was stirred for 1 h at room temperature. The mixture was filtrated through a D_3 frit. The filtrate was reduced to one-third of its original volume under vacuum and kept overnight at −80 °C to yield large

(34) (a) Brookhart, M.; Grant, B., Jr *Organometallics* **1992**, *11*, 3920. (b) Jutzi, P.; Müller, C.; Stammler, A.; Stammler, H. G. *Organometallics* **2000**, *19*, 1442.

(35) Sholte, G.; Meijerink, N. L. J.; Schofelleers, H. M.; Brands, A. M. G. *J. Appl. Polym. Sci.* **1984**, *29*, 3763.

Table 5. Ethylene Polymerization with 3/MAO, Ni(COD)$_2$/PNP (2)/[H(OEt$_2$)$_2$][B(3,5-(CF$_3$)$_2$C$_6$H$_3$)$_4$], and 5/[H(OEt$_2$)$_2$][B(C$_6$F$_5$)$_4$]^a

entry	catalyst system	T (°C)	time (min)	PE yield (g)	productivity ((kg PE) mol^{-1} h^{-1})^b	M_n($\times 10^3$ g mol^{-1})^c	M_n($\times 10^3$ g mol^{-1})^d	M_w/M_n^{d}	T_m^{e} (°C)	branch ^{f}(/1000C)
1	Ni(cod)$_2$/**2**/[H(OEt$_2$)$_2$][B(3,5-(CF$_3$)$_2$C$_6$H$_3$)$_4$]	20	45	0.12	15	4.2	4.2	6.3	nd	7
2	Ni(cod)$_2$/**2**/[H(OEt$_2$)$_2$][B(3,5-(CF$_3$)$_2$C$_6$H$_3$)$_4$]	40	10	0.09	31	2.3	nd	nd	127	10
3	Ni(cod)$_2$/**2**/[H(OEt$_2$)$_2$][B(3,5-(CF$_3$)$_2$C$_6$H$_3$)$_4$]	60	10	0.39	129	7.0	nd	nd	124	14
4	Ni(cod)$_2$/**2**/[H(OEt$_2$)$_2$][B(3,5-(CF$_3$)$_2$C$_6$H$_3$)$_4$]	80	10	0.85	280	3.8	nd	nd	120	9
5	**5**/[H(OEt$_2$)$_2$][B(C$_6$F$_5$)$_4$]	20	30	5.65	349	3.5	3.7	4.2	122	12
6	**5**/[H(OEt$_2$)$_2$][B(C$_6$F$_5$)$_4$]	80	30	2.78	161	2.9	2.9	3.5	122	7
7^g	**5**/[H(OEt$_2$)$_2$][B(C$_6$F$_5$)$_4$]	80	30	1.14	80	2.6	2.5	4.1	120	15

^{a} Polymerization experiments were conducted under 5 atm of ethylene using 30–40 μmol of Ni precursor in 25 mL of toluene (see Experimental Section). ^{b} Average polymerization activity based on polymerization time. ^{c} Determined by H NMR, assuming one C=C per chain. ^{d} Determined by GPC. ^{e} Determined by DSC. ^{f} Determined by ^{1}H NMR, from the relative intensities of CH_3 and CH_2 signals and assuming one Me end per chain.[29] ^{g} Run in chlorobenzene.

purple crystals. The crystals were collected by filtration, washed with pentane, and dried under vacuum to yield a red powder (0.25 g, 61%). Anal. Calcd for $C_{66}H_{78}N_2NiO_8P_4$: C, 65.52; H, 6.50; N, 2.32. Found: C, 65.18; H, 6.75; N, 2.20. Crystals of **4** suitable for single-crystal X-ray diffraction analysis were obtained from a saturated solution of **4** in a 10:1 toluene−pentane solution at −30 °C. The two PNP ligands of **4**, labeled c and d, were distinguished by 2D NMR experiments. ^{1}H NMR (toluene-d_8, 300 MHz, 376 K): δ 7.83 (m, br, 8H, H$_{ortho}$), 6.93 (d, $^3J_{HH}$ = 7.6, 8H, H$_{para}$), 6.42 (d, $^3J_{HH}$ = 7.6, 8H, H$_{meta}$), 3.10 (s, br, 24H, OMe), 2.58 (m, br, 6H, NMe), 2.13 (s, br, 24H, Me). ^{1}H NMR (toluene-d_8, 300 MHz, 230 K): δ 8.73 (m, 4H, H$_{ortho}$), 7.28 (m, 4H, H$_{ortho}$(d)), 7.17 (d, $^3J_{HH}$ = 7.0, H$_{meta}$(c)), 6.87 (d, $^3J_{HH}$ = 6.2, H$_{meta}$(d)), 6.47 (d, $^3J_{HH}$ = 7.0, 4H, H$_{para}$(c)), 6.38 (d, $^3J_{HH}$ = 6.2, 4H, H$_{para}$(d)), 3.18 (s, 12H, OMe(d)), 3.00 (s, 12H, OMe(c)), 2.86 (m, br, 6H, NMe), 2.25 (s, 12H, Me(c)), 2.25 (s, 12H, Me(d)). ^{13}C{^{1}H} (HMBC/HMQC) NMR (toluene-d_8, 75 MHz, 230 K): δ 158.6 (br m, C-6(c)), 156.7 (br m, C-6(d)), 140.8 (br m, C-2(c)), 129.9 (br m, C-4(d)), 129.6 (br m, C-2(d)), 128.7 (br m, C-3(c)), 127.9 (br m, C-3(d)), 126.5 (br m, C-4(c)), 109.6 (br m, C-5(d)), 109.4 (br m, C-5(c)), 53.9 (Me), 31.6 (br m, NMe), 20.9 (OMe(c)), 20.3 (OMe(d)), the C-1 aryl resonances were not observed. ^{31}P{^{1}H} NMR (toluene-d_8, 202 MHz, 298 K): δ 79.9 (br).

{PNP}Ni(cod) (5). A Schlenk flask was charged with **2** (0.200 g, 0.347 mmol) and Ni(cod)$_2$ (0.095 g, 0.347 mmol). Toluene was cannula-transferred in at −80 °C, and the mixture was stirred for 1 h at −80 °C, during which time the initial pale yellow solution became red. The solution was allowed to warm to room temperature and stirred for 2 h. The brown solution was filtered through a D_3 frit and concentrated to dryness under vacuum. The resulting solid was washed with pentane (2 × 5 mL) and dried under vacuum to yield an orange-brown powder (0.210 g, 90%). ^{1}H NMR (C_6D_6, 500 MHz, 298 K): δ 7.85 (m, 4H, H$_{ortho}$), 7.10 (d, $^3J_{HH}$ = 7.8, 4H, H$_{para}$), 6.61 (d, $^3J_{HH}$ = 7.8, 4H, H$_{meta}$), 4.94 (s, 4H, cod-CH), 3.28 (s, 12H, OMe), 2.79 (t, $^3J_{PH}$ = 7.2, 3H, NMe), 2.68 (m, 4H, cod-CH$_2$), 2.59 (m, 4H, cod-CH$_2$), 2.29 (s, 12H, Me). ^{1}H NMR (CD_2Cl_2, 500 MHz, 298 K): δ 7.41 (m, 4H, H$_{ortho}$), 7.09 (d, $^3J_{HH}$= 7.8, 4H, H$_{para}$), 6.72 (d, $^3J_{HH}$ = 7.8, 4H, H$_{meta}$), 4.18 (s, 4H, cod-CH), 3.44 (s, 12H, OMe), 2.35 (m, NMe signal overlap with free cod signal), 2.28 (s, 12H, Me), 2.12 (m, 4H, cod-CH$_2$), 1.97 (m, 4H, cod-CH$_2$). ^{13}C{^{1}H} NMR (C_6D_6, 125 MHz): δ 158.0 (br m, C-6), 133.4 (br m, C-2), 128.5 (br m, C-3), 129.0 (br m, C-4), 124.7 (br m, C-1), 109.9 (br m, C-5), 82.4 (cod-CH), 54.3 (OMe), 31.4 (br m, NMe), 30.5 (cod-CH$_2$), 20.6 (Me). ^{31}P{^{1}H} NMR (CD_2Cl_2, 202 MHz): δ 72.9.

Generation of [{PNP}Ni(codH)][B(C$_6$F$_5$)$_4$] (6). An NMR tube was charged with {PNP}Ni(cod) (**5**) (9.8 mg, 13.2 μmol) and [H(OEt$_2$)$_2$][B(C$_6$F$_5$)$_4$] (11.3 mg, 13.6 μmol), and C_6D_5Cl was vacuum transferred in at −40 °C. The tube was vigorously shaken for 10 s, during which time the solution color changed from orange to dark brown. NMR spectra were recorded at −40 °C. ^{1}H NMR (C_6D_5Cl, 500 MHz, 235 K): all signals were very broad and overlapped with each other. ^{19}F{^{1}H} NMR (C_6D_5Cl, 470 MHz, 235 K): δ −130.6 (br s, 2F, *o*-F) −160.4 (br s, 1F, *p*-F) −164.3 (br s, 2F, *m*-F). ^{31}P{^{1}H} NMR (C_6D_5Cl, 202 MHz, 235 K): δ 53.3 (br s). ESI-MS (CH_2Cl_2): calcd for $^{12}C_{41}{}^1H_{52}{}^{14}N^{16}O_4{}^{30}P_2{}^{56}Ni$: 742.3; found: 742.1.

X-ray Crystallographic Analysis of 3 and 4. Suitable single crystals were mounted onto glass fibers using the "oil-drop" method. Data were collected using a Bruker SMART APEX diffractometer (**3**) or a NONIUS Kappa CCD diffractometer (**4**), both operating with graphite-monochromatized Mo Kα radiation (λ = 0.71073 Å). A combination of ω- and φ-scans was carried out to obtain at least a unique data set. Crystal structures were solved by means of the Patterson method; remaining atoms were located from difference Fourier synthesis, followed by full-matrix least-squares refinement based on F^2 (programs SHELXS-97 and SHELXL-97).[36] Many hydrogen atoms could be found from the Fourier difference.[13] Carbon-bound hydrogen atoms were placed at calculated positions and forced to ride on the attached carbon atom. The hydrogen atom contributions were calculated but not refined. All non-hydrogen atoms were refined with anisotropic displacement parameters. The locations of the largest peaks in the final difference Fourier map calculation as well as the magnitude of the residual electron densities were of no chemical significance. The unit cell of **3** was found to contain three CH_2Cl_2 solvent molecules and that of **4** contained four toluene solvent molecules. Crystal data and details of data collection and structure refinement are given in Table 1. Thermal ellipsoids are drawn at the 50% probability level.

Computational Methods. The gas phase structures of **3**, {PNP}Ni(*n*-propyl)$^+$, and {PNP}Ni(C$_2$H$_4$)(*n*-propyl)$^+$ were optimized using the Turbomole software package using density functional theory (DFT). The geometry optimizations were performed using the B3LYP density functional.[37] All atoms were modeled using the TZVP basis set.[38] The atom coordinates determined in the solid state for **3** were used as a starting point to build {PNP}Ni(*n*-propyl)$^+$ and {PNP}Ni(C$_2$H$_4$)(*n*-propyl)$^+$. For {PNP}Ni(*n*-propyl)$^+$, several conformers that differ in the orientation of the phenyl rings of the PNP ligand were used as a starting point. The most stable structures for these three species are available as Supporting Information as pdb files.

Ethylene Polymerization by Ni(cod)$_2$/2/[H(OEt$_2$)$_2$][B(3,5-(CF$_3$)$_2$C$_6$H$_3$)$_4$] (Table 5, entries 1–6). In a glovebox, a 100 mL high-pressure glass reactor (Top Industrie) was charged with **2**, Ni(cod)$_2$, and [H(OEt$_2$)$_2$][B(3,5-(CF$_3$)$_2$C$_6$H$_3$)$_4$] (30–40 μmol, 1:1:1 ratio). On the vacuum line, toluene (20–30 mL) cooled at −80 °C was added, and the resulting yellow solution was stirred for 5 min at 0 °C. Activation was continued for 5 min at the desired

(36) (a) Sheldrick, G. M., *SHELXS-97, Program for the Determination of Crystal Structures*; University of Goettingen: Germany. 1997. (b) Sheldrick, G. M., *SHELXL-97, Program for the Refinement of Crystal Structures*; University of Goettingen: Germany. 1997.

(37) Becke, A. D. *J. Chem. Phys.* **1993**, *98*, 5648. (b) Lee, C.; Yang, W.; Parr, R. G. *Phys. Rev. B* **1988**, *37*, 785.

(38) Schafer, A.; Huber, C.; Ahlrichs, R. *J. Chem. Phys.* **1994**, *100*, 5829.

(39) *IUPAC compendium of Chemical Terminology* (second edition); 1997, online version, www.iupac.org.

polymerization temperature (20–80 °C). The solution was degassed under vacuum, the reactor was pressurized with ethylene (5 atm), and the mixture was stirred for 10–45 min at the desired temperature (20–80 °C). Ethylene consumption was monitored using an electronic manometer connected to a secondary 100 mL ethylene tank that feeds the reactor by maintaining the total pressure constant. The polymerization was stopped by venting the vessel and adding a 10% HCl solution in methanol (30 mL). The polymer was collected by filtration, washed with methanol and acetone (2 × 15 mL), and dried under vacuum overnight.

Ethylene Polymerization by 5/[H(OEt$_2$)$_2$][B(C$_6$F$_5$)$_4$] (Table 5, entries 5–7). In a glovebox, a 100 mL high-pressure glass reactor (Top Industrie) was charged with **5** and [H(OEt$_2$)$_2$][B(C$_6$F$_5$)$_4$] (30–40 μmol, 1:1 ratio). The reactor was evacuated and pressurized with ethylene (5 atm). Toluene (25 mL) was added at room temperature by syringe under ethylene pressure, and stirring was initiated. The reactor was heated to the desired temperature. The polymer was isolated as described above.

Acknowledgment. This work was supported by the U.S. Department of Energy (DE-FG02-00ER15036), the French Ministère de la Recherche et de l'Enseignement Supérieur (Ph.D. grant to L.L.), Total Petrochemicals (Ph.D. grant to A.S.R.), and the Institut Universitaire de France (fellowship to J.F.C.). We thank Dr. Ian Steele (University of Chicago) and Dr. Loïc Toupet (University of Rennes 1) for the structure determination of **3** and **4**, respectively.

Supporting Information Available: Additional NMR data for **3**, **4**, and **5**, ESI-MS data for **6**, crystallographic data for **3** and **4** as CIF files, and the DFT-optimized structures of **3**, {PNP}Ni(*n*-propyl)$^+$, and {PNP}Ni(C$_2$H$_4$)(*n*-propyl)$^+$ as pdb files. This material is available free of charge via the Internet at http://pubs.acs.org.

OM701215S